Dissociative excitation of SO_2 by electron impact

W. Kedzierski, C. Malone, and J.W. McConkey

Abstract: Dissociative excitation of SO_2 by electron impact to produce excited oxygen fragments, in particular O (^{1}S), has been studied in the energy range from threshold to 400 eV. Three processes leading to O (^{1}S) production have been identified and the positions of the relevant repulsive states of SO_2 in the Franck–Condon region have been determined. The multiplicities and symmetry characteristics of two of these states have also been established. The absolute cross section for production of O (^{1}S) by all channels is measured to be 2.2×10^{-18} cm^2 at 150 eV. The relative cross section for production of O (3p ^{3}P and 3p ^{5}P) from threshold to 400 eV has also been measured. The existence of a hitherto unidentified triplet state of SO_2 that emits in the near infra red has been established.

PACS No.: 34.80Gs

Résumé: Nous avons étudié l'excitation dissociative du SO_2 par impact électronique produisant des fragments d'oxygène excité, en particulier O (^{1}S). Nous avons identifié trois mécanismes de production de O (^{1}S) et avons déterminé la position des états répulsifs pertinents du SO_2 dans la région de Franck–Condon. Nous avons obtenu les multiplicités et les caractéristiques de symétrie de deux de ces états. Notre mesure de la section efficace absolue de production de O (^{1}S) pour tous les canaux donne 2.2×10^{-18} cm^2 à 150 eV. Nous mesurons aussi la section efficace relative de production de O (3p ^{3}P et 3p ^{5}P), du seuil jusqu'à 400 eV. Nous avons découvert un état triplet de SO_2 qui émet dans l'infrarouge proche.

[Traduit par la rédaction]

1. Introduction

Interest in processes involving the dissociation of SO_2 continues for a variety of reasons. It is a major pollutant in the Earth's atmosphere and, as such, information on dissociation pathways and dynamics are relevant to air quality improvement. In addition it is a major constituent in the atmosphere of Jupiter's satellite, Io, [1–3] and has been observed in the atmosphere of Venus [4]. Modelers require as complete information as possible on the various channels and dissociation pathways that are open when electrons and photons interact with ground-state SO_2 molecules. The steady stream of both theoretical and experimental publications that continues is itself a testament to the interest in this molecule and in its break-up. Recently, Kuznetsov et al. [5] studied the removal of SO_2 from stack gas by pulsed electron beam irradiation, Basner et al. [6] and Lindsay et al. [7] measured partial ionization cross sections from threshold to 1000 eV, Shanker and Hippler [8] studied X-ray emission following 3.5–14 keV electron impact, while e-impact cross-section calculations of various kinds have been presented by various researchers [9–11]. Recent relevant works on the photodissociation of SO_2 are those of

Received September 9, 1999. Accepted April 6, 2000. Published on the NRC Research Press Web site on August 25, 2000.

W. Kedzierski, C. Malone, and J.W. McConkey. Department of Physics, University of Windsor, Windsor, ON N9B 3P4, Canada.

Manatt and Lane [12] and Holland et al. [13].

The situation vis-a-vis dissociative excitation by electron impact was reviewed by van der Burgt et al. [14] who gave extensive references to earlier work. Most of the work resulting in excited fragments following electron impact on the parent SO_2 molecule has involved detection of photon emission as the fragments decay. In this connection we mention the work of Ajello and co-workers [15,16] who considered emissions in the spectral range 40–430 nm, Becker et al. [17] whose data covered the range 45–110 nm, Miller and Becker [18] who worked in the 200–550 nm range, and Johnson et al. [19] whose data covered the range 250–400 nm. We note that data covering the important near infrared region where many important emissions of oxygen, for example, lie, are conspicuous by their absence. This is partially remedied in the present study. When the excited fragments are metastable, it is not possible to detect them from their photon emission and so direct detection using some type of surface detector must be used. Such a scheme was used by van der Burgt et al. [14] who used a channel electron multiplier. They observed Rydberg fragments of S, O, and SO but were unable to distinguish between different states or decay channels. Their detector was sensitive to O(^{5}S) metastables, (excitation energy 9.14 eV) but not to O (^{1}S), (excitation energy 4.18 eV). In the present instance we use a special detector, which is selectively sensitive to O (^{1}S) atoms, to study production of this single fragment alone. In this way we are able to greatly simplify the dissociation manifold that is under study.

2. Experimental

The apparatus used in these studies has been described extensively elsewhere, [20–22], and so only a brief outline giving the salient features will be included here. A crossed beam apparatus is used in which a pulsed electron beam and the target gas beam are mutually orthogonal. Fragments formed in the interaction drift to a surface detector located in a separate differentially-pumped region. The detector consists of a layer of xenon continuously deposited on a cold finger held at 65–69 K. When O (^{1}S) atoms impact the Xe surface they thermalize, form XeO excimers and radiate (predominantly a broad band near 725 nm). A cooled photomultiplier detects the emission through a suitable filter. Time-of-flight (TOF) spectra are acquired at a fixed incident electron beam energy or, alternatively, TOF windows are chosen and excitation functions appropriate to data arriving at the detector during those windows are acquired under computer control. The detector has a high quantum efficiency for O (^{1}S) but is completely insensitive to any other species produced in the electron–SO_2 interaction.

3. Results and discussion

Figure 1 shows TOF data taken at an incident energy of 50 eV. The large peak at time zero is due to photons that are produced in the interaction region during the electron beam pulse and which are scattered into the photomultiplier. As such they provide a convenient way of setting the zero of the time scale. A broad peak is then observed at arrival times of approximately 40 μs as the O (^{1}S) atoms arrive at the xenon surface. In Fig. 2 we present data at two energies, 50 and 100 eV. The prompt photon peak, which possesses quite a long tail has been removed from these data for clarity. It can be seen that a second peak appears on the TOF spectrum taken at the higher energy. Thus, from the raw TOF spectra, it is clear that at least two processes are contributing to O (^{1}S) production. The more energetic fragments reaching the detector at the shorter flight times must result from a steeper repulsive surface being accessed in the Franck–Condon region.

Knowing the mass of the detected particle and the distance to the detector it is trivial to convert the TOF data of Fig. 2 to kinetic energy spectra. These are displayed in Fig. 3 where some smoothing of the data has been applied for clarity. The spectra are truncated at energies below 2 eV because of the poor quality of the data at these low energies. Both spectra are observed to possess two peaks, near 3 and 5 eV, with long tails to high energy. At the higher energy electron impact, fragments are observed with energies in excess of 20 eV, again emphasizing the steepness of the repulsive surfaces involved. We note

Fig. 1. TOF spectrum for metastable O (^{1}S) fragments produced by 50 eV electron impact on SO_2. Zero time corresponds to the centre of the 5 μs wide electron pulse. The features due to prompt photons and metastables are indicated.

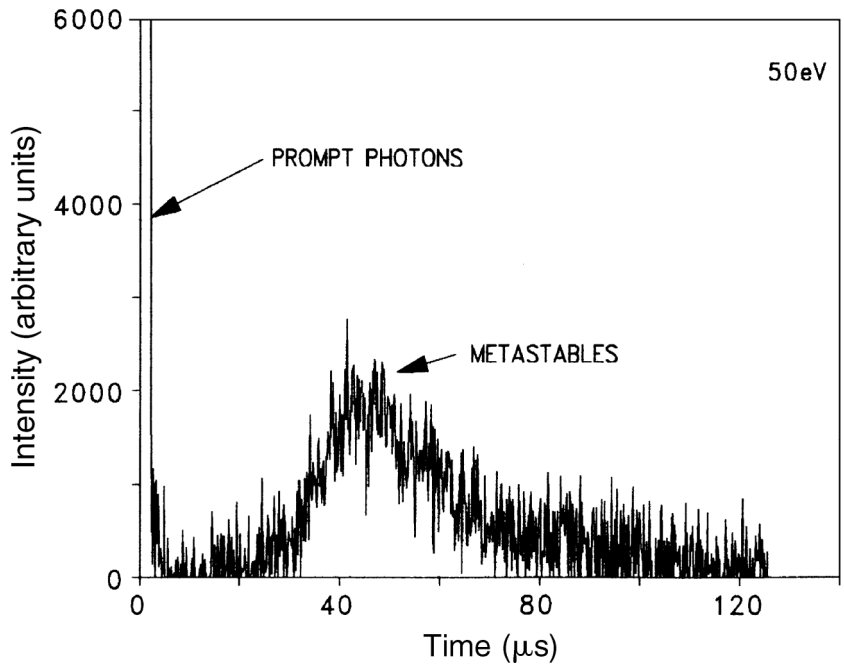

that the 5 eV peak may be correlated with the 40 μs peaks in Fig. 2. Significantly, the 3 eV feature of Fig. 3 arises from the long tails of the TOF spectra where no peak is obvious, whereas the pronounced 30 μs peak, seen in the 100 eV spectrum, correlates with the long tail in the kinetic energy spectrum, the centre of the peak corresponding to an energy of approximately 12 eV. Hence, consideration of both TOF and energy data reveals that at least three processes must be contributing to O (^{1}S) production.

It is evident from Fig. 1 that a significant number of prompt photons are being emitted from the interaction region in the spectral range covered by the red filter in front of the photomultiplier. These photons not only start the clock for TOF acquisition but they also are important for energy calibration as discussed later. To identify the source of these photons we did a spectral scan using a monochromator in place of the filter. The results of this are shown in Fig. 4. This is a low-resolution scan and no attempt has been made to correct for the relative sensitivity of the detection system with wavelength. We note the molecular features below 500 nm that had been observed by previous workers (see Introduction), a number of weak, probably atomic, features between 500 and 700 nm, and a weak background continuum which, as discussed later, is probably due to another emission of SO_2. However, by far the dominant features of the spectrum are the two atomic oxygen lines at 777.4 and 844.7 nm. These correspond to the transitions 3p ^{5}P – 3s ^{5}S and 3p ^{3}P – 3s ^{3}S, respectively. We note that the same intense lines were observed when e–CO_2 collisions were being studied [23]. Using the data listed in ref. 16 it is easy to calculate the adiabatic energies for production of the ^{5}P and ^{3}P states in the simplest break-up process, namely,

$$e + SO_2 \longrightarrow SO(X) + O^* \quad (1)$$

Assuming no vibrational excitation of the SO, these energies are 16.46 and 16.71 eV, respectively. Since

Fig. 2. TOF spectra for O (^{1}S) fragments produced by 50 eV (lower curve) and 100 eV (upper curve) electron impact on SO_2. Note that the prompt photon peaks have been supressed. Some smoothing has been applied to reduce the statistical scatter in the data. A kinetic energy scale, appropriate for O (^{1}S) fragments, is given at the top of the figure.

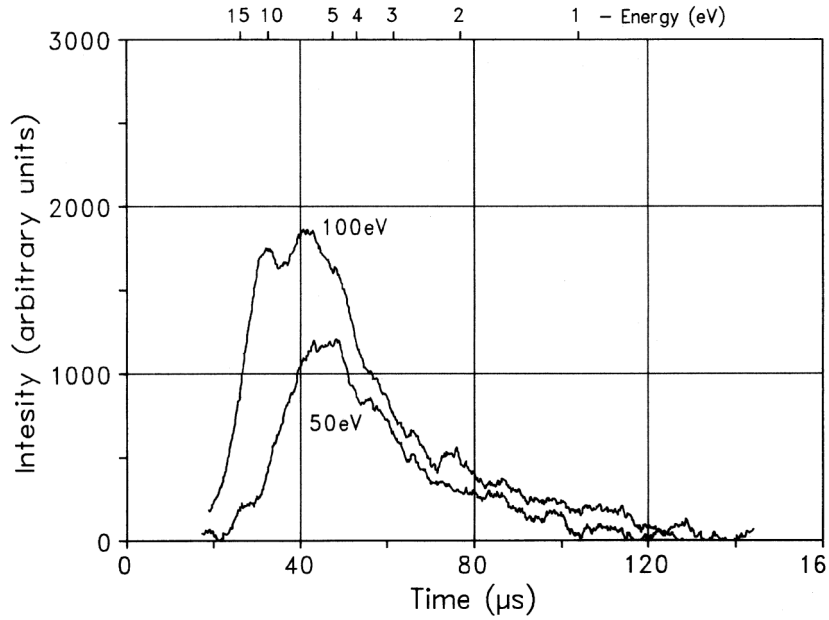

Fig. 3. O (^{1}S) fragment kinetic energy spectra obtained from the data of Fig. 2.

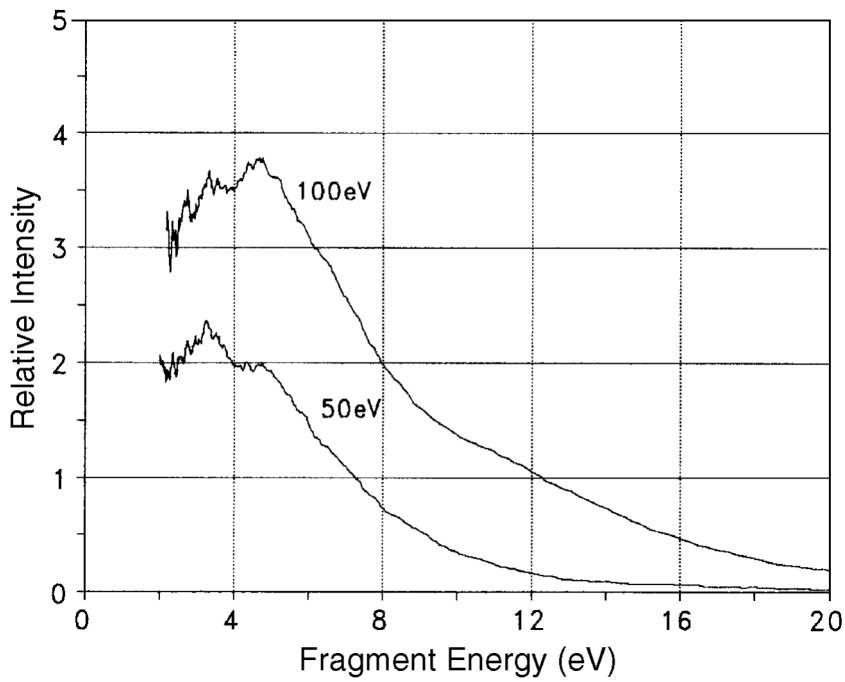

Fig. 4. Low-resolution photon emission spectrum following 100 eV electron impact on SO_2. No attempt has been made to correct the data for any variations of detector system sensitivity with wavelength. See text for discussion.

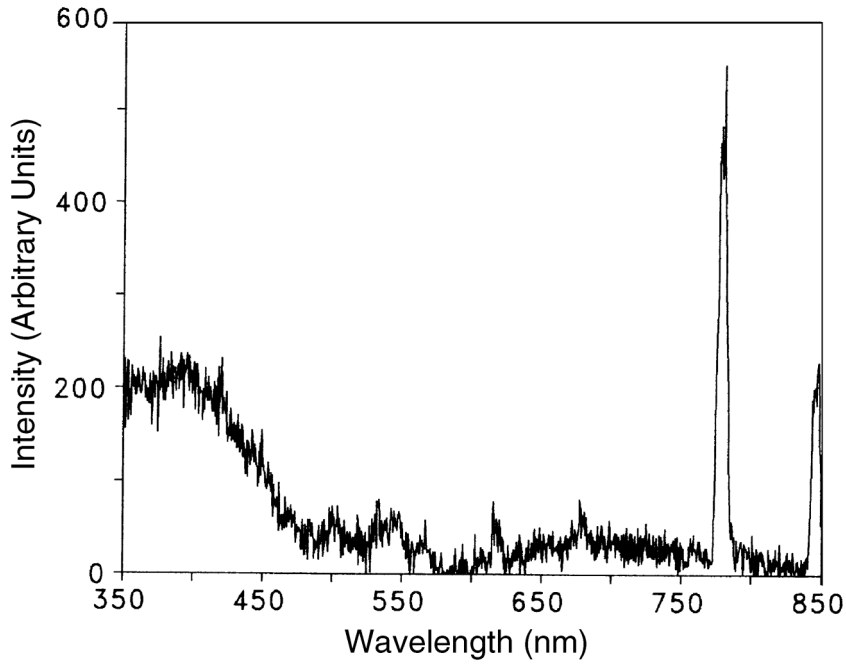

Ajello et al. [16] found that excited oxygen species had threshold excitation energies very close to their calculated adiabatic threshold energies, it seems reasonable to assume that we will have a similar situation and hence be able to use the observed threshold energy of the near infrared lines as an energy calibration point. The energy resolution of our electron gun is about 1 eV and so our measured energies are uncertain by this amount. We find the main threshold for production of O (^{1}S) to occur 0.6 eV below the threshold for the infrared lines, i.e., at 15.9 eV using this calibration. A less pronounced threshold occurs around 14 eV. Since the adiabatic threshold for production of O (^{1}S) in a process similar to (1) is 9.93 eV this would mean a maximum total released kinetic energy of the fragments of around 4 or 6 eV (again assuming no vibrational excitation of the SO fragment). This corresponds to O (^{1}S) kinetic energies of 3 and 4.5 eV. These energies are very close to the peak energies observed (see Fig. 3) suggesting that this analysis is reasonable.

The ground state of SO is X($^3\Sigma^-$) [24] whereas the ground state of SO_2 is $X(^1A_1)$ with an included bond angle of 119.5° [25]. Assuming, as discussed above, that the two main processes involve production of ground state SO X($^3\Sigma^-$) in addition to O (^{1}S) allows us to deduce the possible excited repulsive states of SO_2 using the correlation rules given by Herzberg [25]. Although there are a large number of possible states resulting from the above combination they all have either A_1, A_2, B_1, or B_2 character with singlet, triplet, or quintet multiplicities. As discussed below the singlet multiplicity is preferred. An indication of the multiplicity of the excited SO_2 state can be obtained from the shape of the excitation function for O (^{1}S) production. This is shown in Fig. 5. As can be seen, the function is quite broad with a maximum around 150 eV. There is evidence for a shoulder around 50 eV. Such broad excitation functions are typical of optically allowed parent processes where no change in multiplicity occurs. If this is the case, then the excited SO_2 states will have the same singlet character as the ground state.

Fig. 5. Absolute cross section for production of O (^{1}S) fragments of all energies as a function of impact electron energy.

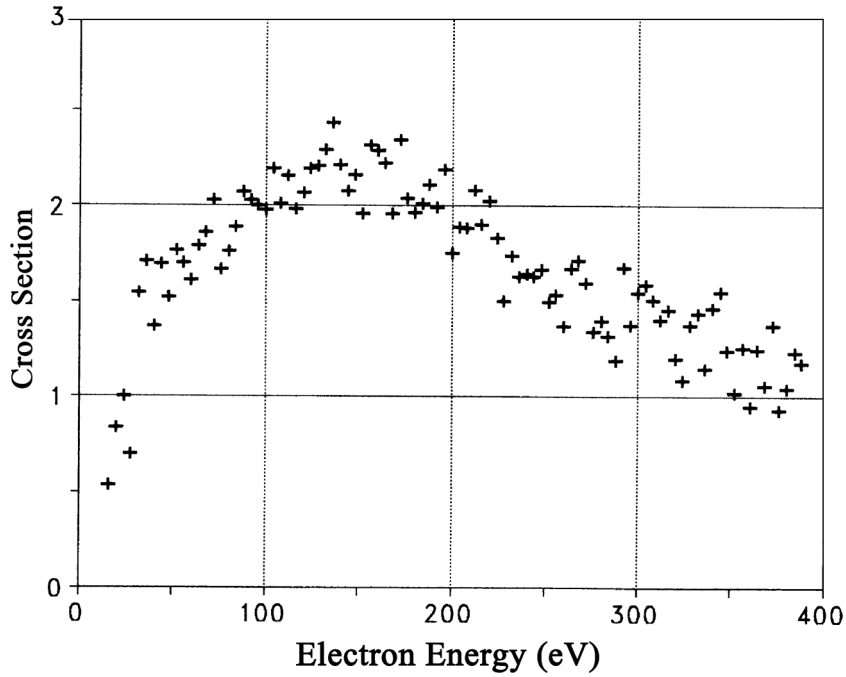

We note that the structure in the curve above 50 eV is consistent with the appearance of an additional production process at about that energy. We recall that Fig. 2 shows evidence of just such a process.

To obtain an absolute calibration for Fig. 5 we use the techniques discussed in earlier publications [20–22]. Basically this is a variation of the so-called "relative flow" technique, where the signal to be calibrated is compared with the signal from a target where the cross section is known. In this case we use CO_2 as the standard since O (^{1}S) flight times are similar for CO_2 and SO_2 targets and the masses are sufficiently similar that differences in the densities of the target gas beams are minimized. Assuming the quoted error of 12% for O (^{1}S) production from CO_2 [21], we estimate an error of 30% for the data of Fig. 5. The maximum cross section at 150 eV is 2.2×10^{-18} cm^2. A significant part of the error arises due to the difficulty of maintaining constant experimental conditions and, in particular, constant detector sensitivity over the long data-taking periods (days).

As a byproduct of the excitation function measurements we present in Fig. 6 the relative excitation function for dissociative excitation of SO_2 to produce the 777.4 and 844.7 nm atomic oxygen lines. As is evident from Fig. 4, these lines dominate the near infrared spectral region. Data were obtained simultaneously with the metastable excitation function data and supplementary data were taken in separate runs using continuous rather than pulsed e-beams. We note that we are unable to provide an absolute calibration for these data but, even so, the shape of the function still provides valuable information. A number of facts should be noted. First it can be seen from the insert to Fig. 6 that, in addition to the main threshold for the strong oxygen lines at 16.5 eV, there is a small feature with a much lower threshold, near 6.5 eV. This is due to the broad molecular feature centered around 700 nm, Fig. 4, and can only be due to an electronic transition in SO_2. Furthermore, the shape of the excitation function in this near-threshold region suggests that excitation of a triplet excited state from the $^1A_1$

Fig. 6. Relative emission cross section for 777.4 and 844.7 nm OI transitions following electron impact on SO_2 . The insert shows the near threshold region in more detail. See text for discussion.

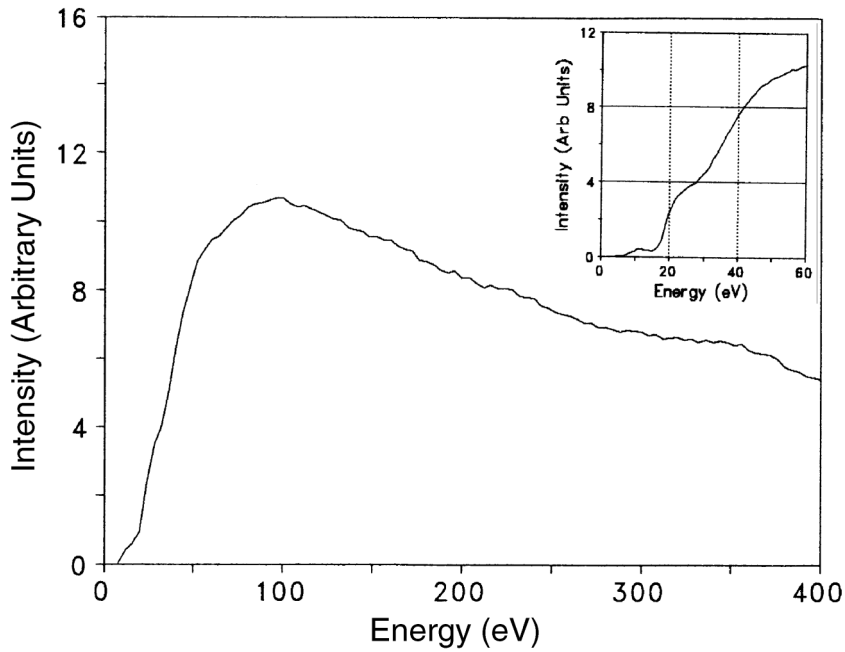

ground state is occurring via an electron exchange process. Vuskovic and Trajmar [26] show strong evidence for excitation of triplet states of SO_2 in their energy loss spectra. It is very possible that what we are observing is emission following a transition between triplet states identified as features "3" and "4" by Vuskovic and Trajmar. Further study of this system is desirable. A second point to notice about the excitation function (Fig. 6) is that there is clearly more than one process contributing to the observed photon production. Clear shoulders are observed near 30 and 50 eV. It is not possible to be specific about which processes are responsible for these as a very large number of total and partial fragmentations, some involving ionization, could be contributing. Finally, since the overall excitation function is broad and essentially structureless, we may conclude that excitation is dominated by optically allowed processes in the parent SO_2 molecule. The maximum in the function occurs near 125 eV, i.e., at about 7.5 times the threshold energy.

4. Conclusions

Measurements of TOF and kinetic energy spectra following dissociative excitation of SO_2 to produce O (^{1}S) fragments have revealed that at least three processes contribute to metastable fragment production. One of these produces very high-energy fragments (10 eV) and originates from a steeply repulsive surface lying more than 50 eV higher in energy in the Franck–Condon region than the ground-state surface. The other two processes dominate the production of O (^{1}S) at lower energies. They produce fragments along with SO X($^3\Sigma^-$) ground-state molecules. Appearance energy measurements position the relevant parent repulsive curves at 14 and 16 eV above the ground-state surface in the Franck–Condon region. The most likely parent states are of $^1A_1$, $^1A_2$, $^1B_1$, or $^1B_2$ character. Measurements involving the near infra red photons produced in the e–SO_2 interaction suggest that excitation of the O 3p ^{5}P and 3p ^{3}P

states are dominant with a background contribution from an unidentified triplet state of SO_2.

Acknowledgements

We are grateful to the Natural Sciences and Engineering Research Council of Canada for financial assistance and to the staff of the mechanical and electronic workshops at the University of Windsor for expert technical assistance.

References

1. J.C. Pearl, R. Hanel, V. Kunde, W. Maguire, K. Fox, S. Gupta, C. Ponnamperuma, and F. Rowland. Nature, **280**, 755 (1979).
2. J.C. Pearl and W.M. Sinton. *In* Satellites of Jupiter. University of Arizona Press, Tucson. 1982.
3. J.T. Clarke, J.M. Ajello, J. Luhmann, N. Schneider, and I. Kanik. J. Geophys. Res. **99E**, 8387 (1994).
4. C.Y. Na, L.W. Esposito, and T.E. Skinner. J. Geophys. Res. **95**, 7485 (1990).
5. D.L. Kuznetsov, G.A. Mesyats, and Y.N. Novoselov. High Temp (Russia), **34**, 833 (1996).
6. R. Basner, M. Schmidt, H, Deutsch, V. Tarnovsky, A. Levin, and K. Becker. J. Chem. Phys. **103**, 211 (1995).
7. B.G. Lindsay, H.C. Straub, K.A. Smith, and R.F. Stebbings. J. Geophys. Res. **101**, 21 151 (1996).
8. R. Shanker and R. Hippler. Z. Phys. D, **42**, 161 (1997).
9. F.A. Gianturco, P. Paioletti, and N. Sanna. J. Phys. B, **30**, 4535 (1997).
10. D. Raj and S. Tomar. J. Phys. B, **30**, 1989 (1997).
11. K.N. Joshipura and M. Vinodkumar. Z. Phys. D, **41**, 133 (1997).
12. S.L. Manatt and A.L. Lane. J. Quant. Spectrosc. Rad. Trans. **50**, 267 (1993).
13. D.M.P. Holland, D.A. Shaw, and M.A. Hayes. Chem. Phys. **201**, 299 (1995).
14. P.J.M. van der Burgt, M.E. Antaya, and J.W. McConkey. Z. Phys. D, **24**, 125 (1992).
15. J.M. Ajello, G.K. James, I. Kanik. J. Geophys. Res. **97A**, 10 501 (1992).
16. J.M. Ajello, G.K. James, I. Kanik, and B.O. Franklin. J. Geophys. Res. **97A**, 10 473 (1992).
17. K. Becker, W.A. van Wijngaarden, and J.W. McConkey. Planet. Space Sci. **31**, 197 (1983).
18. K. Miller, Jr., and K. Becker. Can. J. Phys. **65**, 530 (1987).
19. C.A.F. Johnson, S.D. Kelly, and J.E. Park. J. Chem. Soc. Faraday Trans. 2, **83**, 411 (1987); **83**, 985 (1987).
20. L.R. LeClair and J. W. McConkey. J. Chem. Phys. **99**, 4566 (1993).
21. L.R. LeClair and J. W. McConkey. J. Phys. B, **27**, 4039 (1994).
22. W. Kedzierski, J. Derbyshire, C. Malone, and J.W. McConkey. J. Phys. B, **31**, 5361 (1998).
23. L.R. LeClair. PhD thesis, University of Windsor, Ont. 1993.
24. G. Herzberg. Spectra of diatomic molecules. Van Nostrand, New Jersey. 1950.
25. G. Herzberg. Molecular spectra and molecular structure III. Van Nostrand, New Jersey. 1967.
26. L. Vuskovic and S. Trajmar. J. Chem. Phys. **77**, 5436 (1982).